Published in final edited form as:
Nanomedicine. 2011 August ; 7(4): 435–444. doi:10.1016/j.nano.2010.12.009.

Biodistribution and Pharmacokinetic Analysis of Combination Lonidamine and Paclitaxel Delivery in an Orthotopic Animal Model of Multi-drug Resistant Breast Cancer Using EGFR-Targeted Polymeric Nanoparticles

Lara Milane, MS[1], **Zhen-feng Duan, MD, PhD**[2,3], and **Mansoor Amiji, PhD**[1,*]

[1]Department of Pharmaceutical Sciences, School of Pharmacy, Northeastern University, 360 Huntington Avenue, Boston, MA 02115

[2]Department of Orthopaedic Surgery, Massachusetts General Hospital, Boston, MA 02114

[3]Sarcoma Biology Laboratory, Center for Sarcoma and Connective Tissue Oncology, Massachusetts General Hospital, Boston, MA 02114

Abstract

The aim of this study was to assess the biodistribution and pharmacokinetics of epidermal growth factor receptor (EGFR)-targeted polymer blend nanoparticles loaded with the anticancer drugs lonidamine and paclitaxel. Plasma, tumor, and tissue distribution profiles were quantified in an orthotopic animal model of multi-drug resistant (MDR) breast cancer and were compared to treatment with non-targeted nanoparticles and to treatment with drug solution. Poly(D,L-lactide-co-glycolide)/poly(ethylene glycol)/EGFR targeting peptide (PLGA/PEG/EFGR peptide) construct was synthesized for incorporation in poly(ε-caprolactone) (PCL) particles to achieve active EGFR targeting. An isocratic HPLC method was developed to quantify lonidamine and paclitaxel in mice plasma, tumors, and vital organs. The targeted nanoparticles demonstrated superior pharmacokinetic profile relative to drug solution and non-targeted nanoparticles, particularly for lonidamine delivery. The first target site of accumulation is the liver, followed by the kidneys, and then the tumor mass; maximal tumor accumulation occurs at 3 hours post-administration. Lonidamine/paclitaxel combination therapy administered via EGFR-targeted polymer blend nanocarriers may become a viable platform for the future treatment of MDR cancer.

Keywords

Pharmacokinetics; Multi-drug resistant cancer; nanoparticles; lonidamine; paclitaxel

[*]*CORRESPONDING AUTHOR:* Department of Pharmaceutical Sciences, School of Pharmacy, Northeastern University, 110 Mugar Life Science Building, 360 Huntington Avenue, Boston, MA 02115 Phone: (617) 373-3137, Fax: (617) 373-8886, m.amiji@neu.edu.

CONFLICT OF INTEREST: None

BACKGROUND

The development of multi-drug resistant (MDR) cancer is a barrier to the successful treatment of many clinical cases of cancer. 1–6 MDR refers to a state of resilience against structurally and/or functionally unrelated drugs; MDR can be intrinsic (innate) or acquired through exposure to chemotherapeutic agents. 1 To increase survival potential many MDR cancer cells over-express certain growth factors such as epidermal growth factor (EGF) and corresponding receptors. 7 Epidermal growth factor receptor (EGFR) over-expression results in receptor clustering, which makes these cells hyper-sensitive to EGFR activation and maximizes the effect of EGF. As demonstrated in Figure 1, the current nanocarrier system actively targets the MDR phenotype through the use of a targeting peptide on the surface of the nanocarriers that binds to the EGFR receptor.

As many existing pharmaceutics are less than ideal with respect to parameters such as toxicity and therapeutic index, there is a recognized need to improve these pharmacological features through the design of effective drug delivery systems. The fundamental intent of drug delivery systems is to improve the therapeutic index of biologically active agents 9. The inherent properties of nanotechnology based drug delivery systems make them ideal platforms for achieving this basic aim of drug delivery.

Nanocarriers can enable high drug loading and they can avoid clearance by the reticuloendothelial system (RES). 10 A well established approach to decreasing RES clearance while increasing the circulating plasma concentration and residence time of the nanocarrier is to modify the surface of the nanocarrier with poly(ethylene glycol) (PEG) chains. 11 Active targeting can help a nanocarrier system to overcome biological barriers (active transport verses non-specific endocytosis), decrease the residual toxicity of a system, and increase the therapeutic effect. 12 Multi-functionalization expands the capability of a nanocarrier system where PEG modification, active targeting, multiple therapeutics, and imaging modalities can be combined. 13

This work describes the pharmacokinetic profile and biodistribution of a novel drug delivery system for the treatment of MDR cancer. A primary objective of this system is to actively target EGFR, which is often over-expressed in MDR cancer. As demonstrated in Figure 1, this is achieved by first grafting a PEG-maleimide residue onto poly(D,L-lactide-co-glycolide) (PLGA) and subsequently grafting an EGFR-specific peptide onto the PEG to create a PLGA-PEG-Peptide construct. This construct is then incorporated into the nanoparticle formulation along with PLGA-PEG and poly(ε-caprolactone) (PCL) so that the PLGA and PCL form the core of the particles while the PEG and peptide residues modify the surface of the nanoparticles.

The two therapeutic agents selected for combination therapy are paclitaxel and lonidamine. Although paclitaxel is a common chemotherapeutic agent, its application is often limited by the residual toxicity associated with the drug. Lonidamine is a therapeutic agent with great clinical potential in the treatment of MDR cancer as it acts to inhibit aerobic glycolysis and induce apoptosis. Yet, the clinical application of lonidamine is impeded by the occurrence of residual liver toxicity. The low bioavailability and liver toxicity demonstrated by lonidamine in clinical trials make it an ideal candidate for nanoparticle delivery. Furthermore, combining lonidamine with a low dose of paclitaxel improves the efficacy of both agents.

The biodistribution and pharmacokinetic parameters of a drug/drug delivery system can determine the clinical success of the formulation. The biodistribution and pharmacokinetics of nanoparticle delivered lonidamine are particularly important as lonidamine performed poorly in clinical trials. The biodistribution and pharmacokinetics of lonidamine and paclitaxel administered in EGFR-targeted nanoparticles was compared to administration of

the drugs in non-targeted nanoparticles and to administration of the drugs in solution form. Analysis was performed after 1 hour of administration, 3 hours, 6 hours, and 24 hours.

MATERIALS AND METHODS

Polymer and Peptide Conjugation

The synthesis, detailed methodology, and complete characterization of this nanocarrier system is described in our previous publication. 14 For the synthesis of the PLGA-PEG-peptide construct, an established EGFR specific peptide was used to achieve active targeting with the nanoparticle formulation: YHWYGYTPQNVIGGGGC; the carboxyl terminal cysteine of the peptide reacts with the maleimide of the PLGA-PEG construct. The peptide was synthesized by Tufts University Core Facility, Boston, MA. For the conjugation, 50:50 poly(DL-lactide-*co*-glycolide) (PLGA) with an inherent viscosity of 0.15–0.25 (Durect Lactel® Adsorbable Polymers; Pelham, AL) was used. To synthesize the PLGA-PEG-peptide targeting construct, amine-poly(ethylene glycol) PEG-maleimide (MW 2000; JenKem Technology; Allen, TX) was used, while m-PEG-amine (MW 2000; LaysanBio; Arab, AL) was used to create a (non-targeted) PLGA-PEG construct.

Nanoparticle and Drug Solution Preparations

EGFR targeted and non-targeted polymer blend nanoparticles were synthesized using a solvent displacement method. Poly(ε-caprolactone) (average MW 14.8 kDa; Polysciences, Inc., Warrington, PA) was used as the primary nanoparticle constituent. Briefly, the PLGA-PEG-peptide conjugate (or the PLGA-PEG conjugate for non-targeted particles), PCL, and therapeutic agents were dissolved in 2 mL 50/50 acetonitrile/DMF, and placed in a 37°C water bath for 10 minutes to facilitate dissolution. This polymer/drug solution was added dropwise to 20 mL distilled, deionized water while stirring. The preparation was covered with aerated parafilm, allowed to stir overnight, centrifuged at 10,000g for 30 minutes, and then resuspended in deionized water. To synthesize targeted nanoparticles the PLGA-PEG-peptide conjugate was added to the PCL nanoparticle formulation at 20% w/w total polymer, with an additional 10% w/w of PLGA-PEG conjugate. For the non-targeted nanoparticles, the PLGA-PEG conjugate was added at a concentration of 20% w/w total polymer. Dual agent loaded nanoparticles were synthesized with a 10:1 molar ratio of lonidamine to paclitaxel. Scanning electron microscopy (SEM) images of the nanoparticles were obtained using a Hitachi S-4800 microscope.

Drug solutions for animal treatments were prepared as Cremophor® EL (polyoxyethylated castor oil) stocks. Each mL contained 3 mg paclitaxel, 12 mg lonidamine, 527 mg of Cremophor® EL (BASF, Mount Olive, NJ, USA), and 49.7% (v/v) dehydrated alcohol, USP (Thermo Fisher Scientific, Waltham, MA). Drug solutions for HPLC calibration were prepared in 50:25:25 (v/v) methanol, acetonitrile, water mix. Docetaxel was used as an internal standard at a concentration of 85 μg/ml. Lonidamine and paclitaxel standard curves were prepared at the following concentrations; 200 μg/ml, 40 μg/ml, 8 μg/ml, 1.6 μg/ml, 0.32 μg/ml, 0.2 μg/ml, 0.16 μg/ml, 0.08 μg/ml, and 0.064 μg/ml. To determine the extraction efficiency, organs and plasma from control mice (untreated) were spiked with each concentration of lonidamine and paclitaxel used in the solution standard curve at μg/ml or ug/g of tissue. The y-axis of each calibration curve (data not shown) was plotted as the peak area of drug (lonidamine or paclitaxel) divided by the peak area of docetaxel, while the x-axis was the concentration. The percent recovery was then determined by first dividing the slope of calibration curve in spiked tissue by the slope of the standard curve of drug solution and then multiplying this value by 100.

Cell Culture and Hypoxia

The MDA-MB-231 cells were obtained from ATCC (Manassas, VA). Cells were incubated at 37°C and maintained in RPMI-1640 media (Mediatech, Inc; Manassas, VA) supplemented with 10% fetal bovine serum (Gemini Bio-products; West Sacramento, CA) and 1% penicillin/streptomycin/amphotericin B mixture (Lonza; Walkersville, MD). To create hypoxic conditions using low-oxygen gas; cell culture flasks were placed in a modular incubation chamber (Billups-Rothenberg, Inc.; Del Mar, CA), flushed with a 0.5% O_2, 5% CO_2, nitrogen balanced gas for five minutes, and incubated at 37°C for five days.

Orthotopic Tumor Model Development

The protocol for animal experiments described in this article was approved by Northeastern University's Institutional Animal Care and Use Committee. Female *nu/nu* mice were obtained from Charles River Laboratories (Wilmington, MA) and were housed in sterile cages on a 12:12 light/dark cycle with ad libitum acess to food and water. To establish the xenografts, mice were anesthetized with isoflurane and approximately 2 million human breast cancer cells suspended in a 100 μl of a 50:50 mix of matrigel and serum free medium was injected into the mammary fat pad of the mice using pre-chilled, sterile syringes with 27 gauge, ½" needles. Tumor size was measured every other day using Vernier calipers in two dimensions. Individual tumor volumes (V) were calculated using the formula $V = [\text{length} \times (\text{width})^2]/2$ where length is the longest diameter and width is the shortest diameter perpendicular to length.

Treatment and Tissue Preparation

Once tumors reached 100 mm^3, the animals were selected for experimental treatment. A total of 48 mice were used to assess treatment in the pharmacokinetic study (not including control mice). Mice were randomly allotted to the three treatment groups (paclitaxel and lonidamine loaded EGFR-targeted nanoparticles, paclitaxel and lonidamine loaded non-targeted nanoparticles, and paclitaxel and lonidamine solution). Each group was further divided into four subgroups based on post-administration time points for analysis/animal sacrifice (1 hour, 3 hours, 6 hours, and 24 hours). Data from all four subgroups (1 hour, 3 hours, 6 hours, and 24 hours) was used for plasma and tumor tissue biodistribution analysis and to determine pharmacokinetic parameters; biodistribution in the vital organs was conducted at 1 hour and 6 hours post-administration. Treatment was administered via tail vein injection as a single 125 μL dose of 80 mg/kg lonidamine and 20 mg/kg paclitaxel.

At the established post-administration time points, 4 animals from each of the three treatment groups were euthanized by carbon dioxide inhalation. Pre-sacrifice, blood samples were collected from the mice via retro-orbital bleeding; approximately 200 μL of blood was collected. Before bleeding, the mice were anesthetized by isoflurane inhalation. StatSpin® Microtubes (StatSpin, Inc., Norwood, MA) and capillaries were used for blood collection, and were immediately centrifuged for plasma collection. After euthanasia, the tumor mass, liver, lungs, kidneys, spleen, and heart were harvested and weighed. Tissue and plasma samples were then prepared with adaptations according to established methods for the extraction of lonidamine in preparation for HPLC analysis 19. Organs were first spiked with a solution of the docetaxel internal standard (85 μg/ml or per gram of tissue), then the organs were homogenized in a 10:1 (v/w) ratio of buffer (10 mM Tris, 1mM EDTA, and 10% (v/v) glycerol (pH 7.4)). Samples were then centrifuged for 15 minutes at 16,000*g*, extracted with ethyl acetate at a 1:2 (v/v) ratio, evaporated under nitrogen, and resuspended in 100μl of 50:25:25 (v/v) methanol, acetonitrile, water. Plasma samples were collected from the StatSpin® Microtubes and acidified with 1M HCL at a ratio of 1.5:1 (v/v). The sample was then extracted with ethyl acetate at a (v/v) ratio of 1:1.3, evaporated under

nitrogen, and re-suspended in the initial plasma volume of 50:25:25 (v/v) methanol, acetonitrile, water.

HPLC Method Development and Analysis

The HPLC method was developed as an adaptation of established methods for lonidamine and paclitaxel quantification. An isocratic, reversed-phase HPLC method was developed using a SunFire C_{18} Column (5 μm particle size, 4.6×250 mm) (Waters; Milford, MA). The system used was a Waters system (Separations Module, 2695; Waters Corporation, Milford, MA) consisting of two pumps, an autosampler, and UV-detector (Model 2487). The user interface consisted of Waters Empower chromatography data software, which was used for instrument management, data acquisition, and processing. The mobile phase consisted of acetonitrile and water (51:49, v/v) containing 0.1% trifluoracetic acid. The column was equilibrated at a flow rate of 1 mL/min. The elution was monitored at 230 nm. The sample injection volume was 80 μl. HPLC glass vial inserts (Waters; Milford, MA) were used for samples with low volume yields.

Pharmacokinetic Parameter Data Analysis

Pharmacokinetic parameters were determined by using a recently published, free Microsoft Excel add-in, “PKSolver”. The specifications of this program as well as validation was published in the January 2010 edition of *Computer Methods and Programs in Biomedicine*. 21 Non-compartmental analysis was used to determine the pharmacokinetic parameters.

Preparation of Dye-Loaded Nanoparticles and Animal Imaging

Nanoparticles were loaded at 1% w/w with the near IR fluorescent dye DiR (Invitrogen; Carlsbad, CA). The loading efficiency of both non-targeted and targeted nanoparticles was between 65–70% as determined by measuring the supernatant intensity of six nanoparticle batches relative to a standard curve of DiR near infra-red fluorescence. There was also minimal release of the dye from the nanoparticles in PBS for up to 24 hours. The nanoparticles were administered at the same w/v ratio as the paclitaxel/lonidamine combination nanocarriers (20 mg nanoparticle polymer/ 125 μl).

This study used 14 female athymic mice with 100 mm^3 tumors established in the mammary fat pad. Seven mice were injected with each formulation; non-targeted nanoparticles loaded with DiR or EGFR-targeted nanoparticles loaded with DiR. Imaging was done at the following post-administration time points; 15 minutes, 30 minutes, 1 hour, 2 hours, 3 hours, 4 hours, and 6 hours. At the established time points, mice were euthanized via carbon dioxide inhalation and rapidly imaged using a Kodak FX Imaging Station (Rochester, NY). Fluorescent fields were directly overlaid on the x-ray images using the Kodak software.

Statistical Analysis and Graphing

All graphs were made using GraphPad Prism® Software. The plasma concentration and tumor concentration graphs were plotted as mean and coefficient of variation (%) values of data obtained from HPLC analysis; the biodistribution data was plotted as mean and standard deviation values. For each data point, n=4. GraphPad Prism® Software was also used to analyze data and determine significance by using one-way ANOVA and Tukey's Multiple Comparison Test.

RESULTS

Nanoparticle Characterization

As demonstrated by the SEM images in Figure 1, both the targeted and the non-targeted nanoparticles had a smooth spherical shape and an average size of 120–160 nm. The nanoparticles were also characterized by dynamic light scattering, zeta potential measurements, drug loading efficiency, drug release kinetics, ESCA surface analysis, and EGFR-targeting ability; these results are described in our previous publication. 14

Analysis of Lonidamine and Paclitaxel

Using this HPLC method, the retention time of docetaxel was approximately 14.5 minutes, while it was approximately 21.4 minutes for lonidamine, and approximately 17.8 minutes for paclitaxel. Figure 2.A. and 2.B. presents the chromatographs of the highest (200 μg/ml) and lowest (64 ng/ml) concentration of lonidamine detectable in solution. Figure 2.E. is the chromatograph of docetaxel, the internal standard, at a concentration of 85 μg/ml. Figure 2.C. and 2.D. presents the chromatographs of the highest (200 μg/ml) and lowest (160 ng/ml) concentration of paclitaxel detectable in solution. The lowest detectable concentration of lonidamine was 64 ng/ml (0.064 μg/ml); this represents 0.004% of the total administered dose of lonidamine. The lowest detectable concentration of paclitaxel was 160 ng/ml (0.16 μg/ml); this represents 0.04% of the total administered dose of paclitaxel. The percent recovery values from each tissue are listed in Figure 2.F; all values were at or above 87%. There was no significance between the percent drug recovery from the three treatment groups; as such, only the values for targeted nanoparticles are shown in Figure 2.

Biodistribution and Pharmacokinetics Analysis

The plasma concentrations of lonidamine and paclitaxel over the time course of 1 to 24 hours are plotted in Figure 3.A. At 1 hour, 3 hours, and 6 hours post-administration, there was no significance between the plasma concentration of drug solutions and nanoparticles. However, only lonidamine delivered in targeted nanoparticles and non-targeted nanoparticles was detectable after 24 hours. Both drugs and all formulations follow the pattern of an initially high plasma concentration (at 1 hour post-administration) with a steep decline at 3 hours and 6 hours post-administration. The tumor concentrations of lonidamine and paclitaxel administered as a drug solution, in EGFR-targeted nanocarriers, and in non-targeted nanocarriers are depicted in Figure 3.B. At 1 hour post administration there were low concentrations of both lonidamine and paclitaxel for each treatment. At three hours post-administration there was a steep increase for both the lonidamine and paclitaxel concentrations for both the non-targeted and targeted nanoparticles; whereas 1 hour was the T_{max} for drug solution and by three hours post-administration there was a decline in both the paclitaxel and lonidamine concentration. As indicated by the asterisk in Figure 3.B., there was significance between the concentration of lonidamine and paclitaxel administered as solution and the concentration of both drugs administered in non-targeted nanoparticles and in targeted nanoparticles at the three hour time point. There was no significance, however, between either nanoparticle formulation. At six hours post-administration the level of lonidamine administered as solution was below the detection limit of the HPLC method while the paclitaxel concentration approached the limit of detection. At six hours post-administration there was a decline in the concentrations of both drugs for both nanoparticle formulations, and this decline continued until 24 hours post-administration. From this data, it appears that both the non-targeted and the targeted nanoparticles are effective at increasing the tumor concentration of paclitaxel and lonidamine relative to drug solution.

The pharmacokinetic parameters for both plasma and tumor data are presented in Table 1 and Table 2, respectively. Nine parameters were calculated; the terminal elimination rate

constant (λ_z), the half-life ($T_{½}$), the time of maximal concentration (T_{max}), the maximal concentration (C_{max}), the area under the curve ($AUC_{0-\infty}$), the area under the moment curve ($AUMC_{0-\infty}$), the mean residence time ($MRT_{0-\infty}$), the total body clearance (Cl_t), and the volume of distribution (V_d). The asterisk symbols (*) represent significance between drug solution and either non-targeted nanoparticles or targeted nanoparticles, while the double dagger symbols (‡) represent significance between the two nanoparticle formulations. As demonstrated, there was significance for the λ_z between paclitaxel administered in solution and paclitaxel administered in both nanoparticle systems. There was no significance between the plasma $T_{½}$ of paclitaxel solution compared to nanoparticle treatments yet there was significance between the plasma $T_{½}$ of lonidamine solution (1.67 hours) and lonidamine administered in EGFR-targeted nanoparticles (4.16 hours). There was significance between the plasma $AUC_{0-\infty}$values of paclitaxel in solution and paclitaxel delivered in non-targeted nanoparticles. There was also significance between the plasma $AUC_{0-\infty}$values of lonidamine in solution and lonidamine delivered in both nanoparticle formulations as well as significance between the two nanoparticle formulations. For both drugs, there was significance between solution drugs and nanoparticle delivered drugs as well as significance between the two nanoparticle formulations for the $AUMC_{0-\infty}$values. The only significance for the $MRT_{0-\infty}$ was between lonidamine in solution and lonidamine delivered in targeted nanoparticles. The $MRT_{0-\infty}$ of paclitaxel ranged from 1.62 hours (solution) to 2.75 hours (non-targeted nanoparticles), while the $MRT_{0-\infty}$ of lonidamine ranged from 2.36 hours (solution) to 4.38 hours (targeted nanoparticles). Collectively, nanoparticle delivery increases the plasma $AUC_{0-\infty}$ and plasma $AUMC_{0-\infty}$for both drugs and the targeted nanoparticles increase the plasma $MRT_{0-\infty}$ and $T_{½}$ of lonidamine relative to lonidamine administered as solution.

The tumor pharmacokinetic parameters are listed in Table 2. There was a significant decrease in the tumor λ_z between paclitaxel and lonidamine administered in nanoparticle form relative to drug solution. The targeted nanoparticles increased the tumor $T_{½}$ for paclitaxel to 8.24 hours ($p<0.0001$) relative to solution (1.31 hours) while the non-targeted nanoparticles increased the $T_{½}$ to 5.92 hours ($p<0.05$). The targeted nanoparticles also increased the tumor $T_{½}$ of lonidamine to 5.39 hours ($p<0.05$) while the $T_{½}$ of lonidamine in solution was 1.09 hours. Nanoparticle delivery increased the tumor C_{max} of lonidamine from 1.15 μg/ml for solution to 7.38 μg/ml ($p<0.0001$) for targeted nanoparticle delivery, and to 5.68 μg/ml ($p<0.0001$) for non-targeted nanoparticle delivery. Both nanoparticle formulations significantly increased the tumor $AUC_{0-\infty}$ for lonidamine (relative to solution) while only the targeted nanoparticles significantly increased the $AUC_{0-\infty}$ for paclitaxel relative to solution. Both nanoparticle formulations increased the tumor $AUMC_{0-\infty}$ for both drugs relative to drug solution. The targeted nanoparticles significantly increased the tumor $MRT_{0-\infty}$ of paclitaxel from 2.15 hours for solution to 11.45 hours ($p<0.0001$) while the non-targeted nanoparticles increased this time to 7.75 hours ($p<0.0001$). The targeted nanoparticles also significantly increased the tumor $MRT_{0-\infty}$ of lonidamine from 1.94 hours for solution to 7.25 hours ($p<0.0001$). Both nanoparticle formulations significantly decreased the Cl_t and V_d for lonidamine. Collectively, the non-targeted nanoparticles decrease the tumor λ_z of paclitaxel and lonidamine, increase the tumor $T_{½}$ and $MRT_{0-\infty}$ of paclitaxel, increase the C_{max} of lonidamine, decrease the Cl_t and V_d of lonidamine, and increase the $AUMC_{0-\infty}$ for both paclitaxel and lonidamine relative to drug solution. The targeted nanoparticles decrease the tumor λ_z of paclitaxel and lonidamine, increase the tumor $T_{½}$ and tumor $MRT_{0-\infty}$ of both drugs, increase the C_{max} of lonidamine, increase the $AUC_{0-\infty}$ and $AUMC_{0-\infty}$ for both drugs, and decrease the Cl_t and V_d of lonidamine relative to drug solution. Both nanoparticle formulations improve the tumor pharmacokinetic parameters relative to drug solution, with the targeted nanoparticles providing a slight advantage for the pharmacokinetic parameters of combination therapy relative to the non-targeted nanoparticles ($T_{½}$, $AUC_{0-\infty}$, $AUMC_{0-\infty}$, and $MRT_{0-\infty}$).

The biodistribution of lonidamine and paclitaxel at one hour post-administration and six hours post-administration are graphed in Figure 3.C. and Figure 3.D.. The organs analyzed include the liver, lung, kidney, spleen, and heart. There was no significance between solution and nanoparticle treatments for both drugs, at both time points, in all of the organs.

Qualitative Biodistribution Analysis

To further assess the biodistribution of the nanoparticles, a qualitative imaging study was completed using 14 mice. Non-targeted and targeted nanoparticles loaded with DiR (near-IR) dye were administered via tail vein injection and the biodistribution was visualized after 15 minutes, 30 minutes, 1 hour, 2 hours, 3 hours, 4 hours, and 6 hours. The top panel of Figure 4 represents the biodistribution of non-targeted nanoparticles while the biodistribution of the targeted nanoparticles is represented in the bottom panel. The highest near-IR intensity (5806) is indicated by white regions while purple represents an intensity of zero as indicated by the color-scale. For each time point, there does not appear to be a significant difference between the biodistribution of the non-targeted and targeted nanoparticles. At each time point there is also a relatively high accumulation of the dye in the tail; this is most likely due to residual nanoparticles at the site of administration that did not enter the tail vein. At 15 minutes, there is a slight accumulation of fluorescence in the mid-abdominal/liver region (blue). By 30 minutes there is apparent liver accumulation (higher for the non-targeted nanoparticles), with some off-target accumulation of the targeted nanoparticles. By one hour there is much higher liver accumulation of both nanocarriers. By two hours there is apparent kidney accumulation with a slight accumulation in the tumor (breast tissue). By three hours there is higher tumor accumulation for both formulations and low kidney accumulation for the non-targeted nanoparticles. This high level of tumor accumulation is sustained at four hours but is substantially decreased by six hours. This study provides some insight to the behavior of the nanoparticles *in vivo* and is comparable to the biodistribution of the drugs measured using HPLC. The first target site of accumulation is the liver, followed by the kidneys, and then the tumor mass. This study was conducted as a visual complement to the quantitative HPLC study.

DISCUSSION

The mechanisms of targeting nanocarriers to a particular disease are generally categorized as either active or passive targeting strategies. 12 Active targeting involves the use of disease-specific targeting ligands such as antibodies (antigen targeting), lectins (carbohydrate targeting), and peptides (receptor targeting). 12 Active targeting has the ability to improve the therapeutic index of biologically active agents by increasing target-site accumulation and by improving the pharmacokinetics of the system/drugs.

In this study, both the non-targeted and the targeted nanoparticles provided a biodistribution and pharmacokinetic advantage relative to drug solution. The quantitative and qualitative biodistribution profiles of both nanoparticle formulations were almost identical. This illustrates that the minute difference between the two formulations (approximately 2% surface modification with the EGFR peptide) is not enough to alter the biodistribution of the polymer blend nanocarriers. This peptide modification was, however, enough to alter the pharmacokinetic profile of the nanocarriers. For the tumor pharmacokinetics, relative to drug solution, both nanoparticle formulations; decreased the λ_z for both drugs, increased the $T_{½}$ and $MRT_{0\text{-}\infty}$ of paclitaxel, increased the C_{max} of lonidamine, and decreased the Cl_t and V_d of lonidamine. On the other hand, only the targeted nanoparticles (not the non-targeted nanoparticles), significantly increased the plasma and tumor half-life and mean residence time of lonidamine. The primary advantage of EGFR-targeted nanoparticles relative to non-targeted nanoparticles is an improvement in lonidamine pharmacokinetics, in both the plasma and tumor tissue.

In this study, active targeting is beneficial for lonidamine delivery. This result is very important to consider when designing and evaluating drug delivery systems, as active targeting may confer a clinical advantage for the delivery of some agents while it may not lead to any improvement for other pharmaceuticals. Active targeting does not guarantee improved pharmacokinetics. However, for this particular combination therapy, active EGFR targeting improves the pharmacokinetics of the system relative to both drug solution and non-targeted nanoparticles.

An important and often overlooked aspect of active targeting is the clinical translation. For the successful transition of actively targeted nanocarriers from the bench-top to the clinic, there must also be paralleled progression in the clinical characterization of tumors. Before administering a targeted therapy, the phenotype of a patients tumor must be characterized; i.e. EGFR positive or negative. Unfortunately, relative to the rapid rate of actively-targeted treatment development, the progress in improving tumor phenotyping has been slow. This progress is vital to the application of targeted therapies.

In summary, an isocratic HPLC method was developed for the detection and quantification of lonidamine and paclitaxel in mice plasma, tumor tissue, liver, kidney, lung, spleen, and heart. The method was used to compare combination therapy with lonidamine/paclitaxel solution, EGFR-targeted nanoparticles loaded with lonidamine and paclitaxel, and non-targeted nanoparticles. Both nanocarrier formulations demonstrated improved biodistribution and pharmacokinetic parameters relative to drug solution. However, the targeted nanoparticles provided a slight advantage over the non-targeted nanoparticles with regard to some key pharmacokinetic parameters ($T_{½}$, $AUC_{0-\infty}$, $AUMC_{0-\infty}$, and $MRT_{0-\infty}$). A qualitative imaging study of targeted and non-targeted nanoparticles loaded with a near-IR dye demonstrated that the nanocarrier biodistribution profiles progress from liver accumulation, to kidney accumulation, and finally to tumor accumulation; with maximal tumor accumulation between 3–4 hours post-administration. These studies demonstrate that non-targeted and targeted nanoparticles improve the pharmacokinetics of lonidamine/paclitaxel combination therapy relative to solution treatment, and that EGFR-targeted nanoparticles improve the plasma and tumor half-life and mean residence time of lonidamine relative to non-targeted nanoparticles. This drug delivery system may be a promising platform for the future treatment of MDR cancer.

Acknowledgments

Scanning electron microscopy images were acquired with the assistance of Mr. William Fowle at Northeastern University's Electron Microscopy Center. Additionally, Mr. Husain Attarwala of Northeastern University is kindly thanked for his help with the animal model development and *in vivo* studies.

FUNDING SUPPORT: This study was supported by the National Cancer Institute, National Institutes of Health through grants R01 CA-119617 and R01 CA-119617S1 (ARRA Supplement), and R21 CA-135594.

REFERENCES

1. Harris AL, Hochhauser D. Mechanisms of multidrug resistance in cancer treatment. Acta Oncol. 1992; 31:205–213. [PubMed: 1352455]
2. Jamroziak K, Robak T. Pharmacogenomics of MDR1/ABCB1 gene: the influence on risk and clinical outcome of haematological malignancies. Hematology. 2004; 9:91–105. [PubMed: 15203864]
3. Leighton JC Jr, Goldstein LJ. P-glycoprotein in adult solid tumors. Expression and prognostic significance. Hematol Oncol Clin North Am. 1995; 9:251–273. [PubMed: 7642464]
4. Tredan O, Galmarini CM, Patel K, Tannock IF. Drug resistance and the solid tumor microenvironment. J Natl Cancer Inst. 2007; 99:1441–1454. [PubMed: 17895480]

5. Tsuruo T, Naito M, Tomida A, Fujita N, Mashima T, Sakamoto H, Haga N. Molecular targeting therapy of cancer: drug resistance, apoptosis and survival signal. Cancer Sci. 2003; 94:15–21. [PubMed: 12708468]
6. Yague E, Arance A, Kubitza L, O'Hare M, Jat P, Ogilvie CM, Hart IR, Higgins CF, Raguz S. Ability to acquire drug resistance arises early during the tumorigenesis process. Cancer Res. 2007; 67:1130–1137. [PubMed: 17283147]
7. Rojo F, Albanell J, Rovira A, Corominas JM, Manzarbeitia F. Targeted therapies in breast cancer. Semin Diagn Pathol. 2008; 25:245–261. [PubMed: 19013891]
8. Hsieh MY, Yang S, Raymond-Stinz MA, Steinberg S, Vlachos DG, Shu W, Wilson B, Edwards JS. Stochastic simulations of ErbB homo and heterodimerisation: potential impacts of receptor conformational state and spatial segregation. IET Syst Biol. 2008; 2:256–272. [PubMed: 19045821]
9. Kingsley JD, Dou H, Morehead J, Rabinow B, Gendelman HE, Destache CJ. Nanotechnology: a focus on nanoparticles as a drug delivery system. J Neuroimmune Pharmacol. 2006; 1:340–350. [PubMed: 18040810]
10. Batrakova EV, Kabanov AV. Pluronic block copolymers: evolution of drug delivery concept from inert nanocarriers to biological response modifiers. J Control Release. 2008; 130:98–106. [PubMed: 18534704]
11. Moghimi SM, Hunter AC, Murray JC. Long-circulating and target-specific nanoparticles: theory to practice. Pharmacol Rev. 2001; 53:283–318. [PubMed: 11356986]
12. Sinha R, Kim GJ, Nie S, Shin DM. Nanotechnology in cancer therapeutics: bioconjugated nanoparticles for drug delivery. Mol Cancer Ther. 2006; 5:1909–1917. [PubMed: 16928810]
13. Jabr-Milane LS, van Vlerken LE, Yadav S, Amiji MM. Multi-functional nanocarriers to overcome tumor drug resistance. Cancer Treat Rev. 2008; 34:592–602. [PubMed: 18538481]
14. Milane LJ, Duan Z, Amiji MM. Development of EGFR-Targeted Polymer Blend Nanocarriers for Paclitaxel/Lonidamine Delivery to Treat Multi-Drug Resistance in Human Breast and Ovarian Tumor Cells. Mol Pharm. 2010
15. Li Z, Zhao R, Wu X, Sun Y, Yao M, Li J, Xu Y, Gu J. Identification and characterization of a novel peptide ligand of epidermal growth factor receptor for targeted delivery of therapeutics. Faseb J. 2005; 19:1978–1985. [PubMed: 16319141]
16. Song S, Liu D, Peng J, Sun Y, Li Z, Gu JR, Xu Y. Peptide ligand-mediated liposome distribution and targeting to EGFR expressing tumor in vivo. Int J Pharm. 2008; 363:155–161. [PubMed: 18692120]
17. Chawla JS, Amiji MM. Biodegradable poly(epsilon -caprolactone) nanoparticles for tumor-targeted delivery of tamoxifen. Int J Pharm. 2002; 249:127–138. [PubMed: 12433441]
18. Shenoy DB, Amiji MM. Poly(ethylene oxide)-modified poly(epsilon-caprolactone) nanoparticles for targeted delivery of tamoxifen in breast cancer. Int J Pharm. 2005; 293:261–270. [PubMed: 15778064]
19. Grippa E, Gatto MT, Leone MG, Tita B, Adbel-Haq H, Vitalone A, Silvestrini B, Saso L. Analysis of lonidamine in rat serum and testis by high performance liquid chromatography. Biomed Chromatogr. 2001; 15:1–8. [PubMed: 11180293]
20. Ganta S, Amiji M. Coadministration of paclitaxel and curcumin in nanoemulsion formulations to overcome multidrug resistance in tumor cells. Mol Pharm. 2009; 6:928–939. [PubMed: 19278222]
21. Zhang Y, Huo M, Zhou J, Xie S. PKSolver: An add-in program for pharmacokinetic and pharmacodynamic data analysis in Microsoft Excel. Comput Methods Programs Biomed. 2010

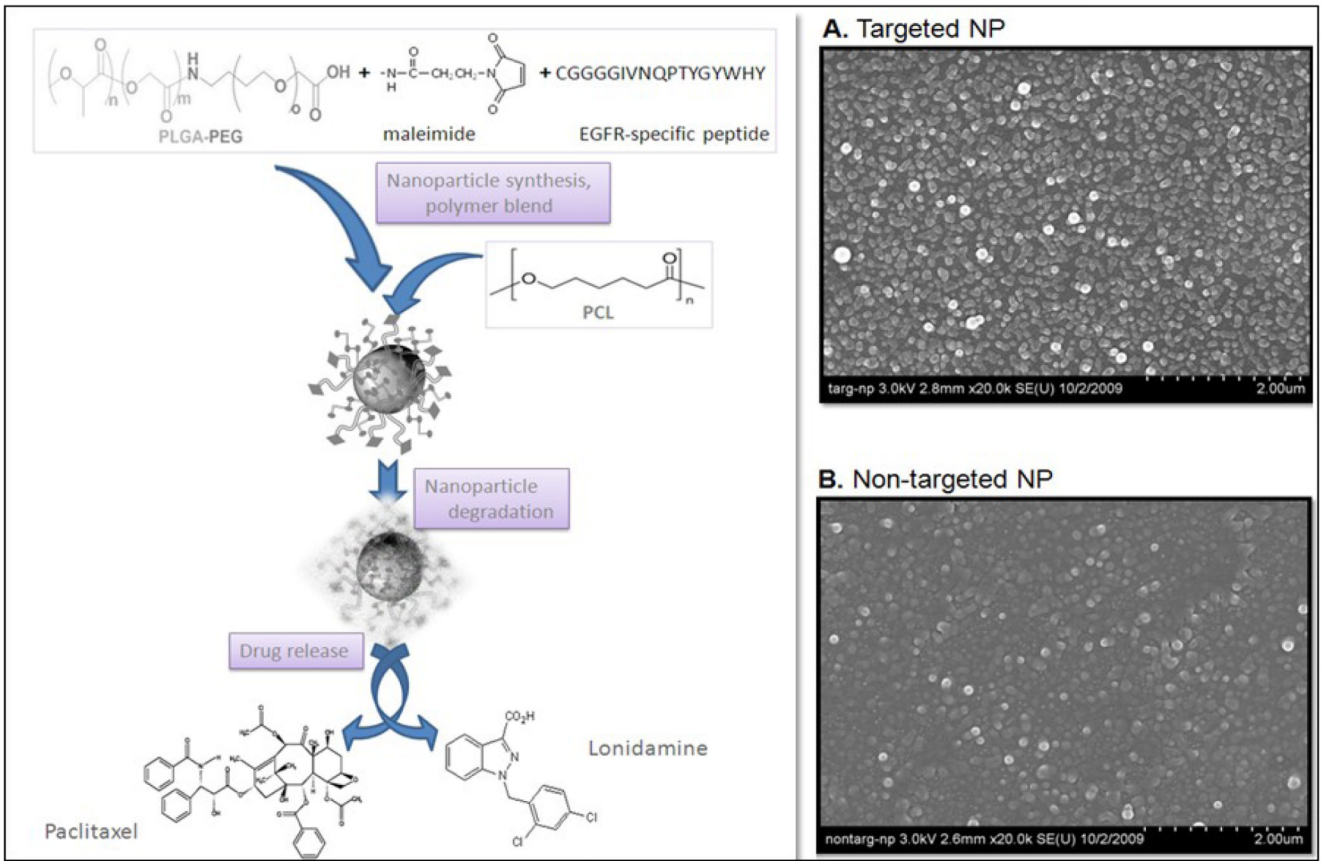

Figure 1.

Schematic illustration of EGFR-targeted polymeric nanocarriers and scanning electron micrographs (SEM) of targeted polymer blend nanoparticles (A) and control (non-targeted) polymer blend nanoparticles (B). The scale bar in the SEM images is 2 μM. The nanocarrier schema is a simplification of conjugation chemistry to illustrate terminal drug release and the use of maleimide as a linker for peptide addition (amine-PEG-maleimide was used).

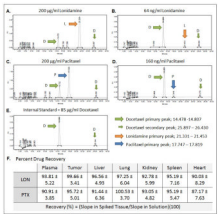

Figure 2.

Reverse phase HPLC analysis of lonidamine and paclitaxel. Docetaxel was used as an internal standard (85 μg/ml). The large green arrow represents the docetaxel primary peak (14.478–14.807), the small green arrow represents the secondary docetaxel peak (25.897–26.430), the large orange arrow represents the primary lonidamine peak (21.331–21.453), and the large blue arrow represents the primary paclitaxel peak (17.747–17.819). Nanoparticle encapsulation did not alter any drug peaks. As indicated in **panel A** and **C**, the highest dose of both lonidamine and paclitaxel (200 μg/ml) were detected with this method. The lower limit of detection for lonidamine was 64 ng/ml (**panel B**) while the lower limit of paclitaxel detection was 160 ng/ml (**panel D**). **Panel E** demonstrates the docetaxel spectra. **Panel F** displays the percent drug recovery values for EGFR-targeted nanoparticles in the seven tissues examined.

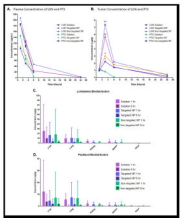

Figure 3.

Plasma and tumor drug concentrations versus time profiles and tissue biodistribution. Mice were treated with either lonidamine/paclitaxel drug solution, non-targeted nanoparticles loaded with lonidamine and paclitaxel, or targeted nanoparticles loaded with lonidamine and paclitaxel. After 1 hour, 3 hours, 6 hours, and 24 hours drug concentrations in the plasma (**Panel A**) and tumors (**Panel B**) was measured. Each data point represents an n= 4 and is graphed as mean and %CV. As indicated by the asterisk in **Panel B**, for both drugs, there was significance between solution administration and administration with both nanocarrier formulations at the three hour time point (**p<0.01, *p<0.05). The biodistribution of lonidamine (**Panel C**) and paclitaxel (**Panel D**) at one hour post-administration and six hours post-administration was quantified in the liver, lung, kidney, spleen, and heart of the three treatment groups. Each bar represents an n=4 graphed as the mean and SD.

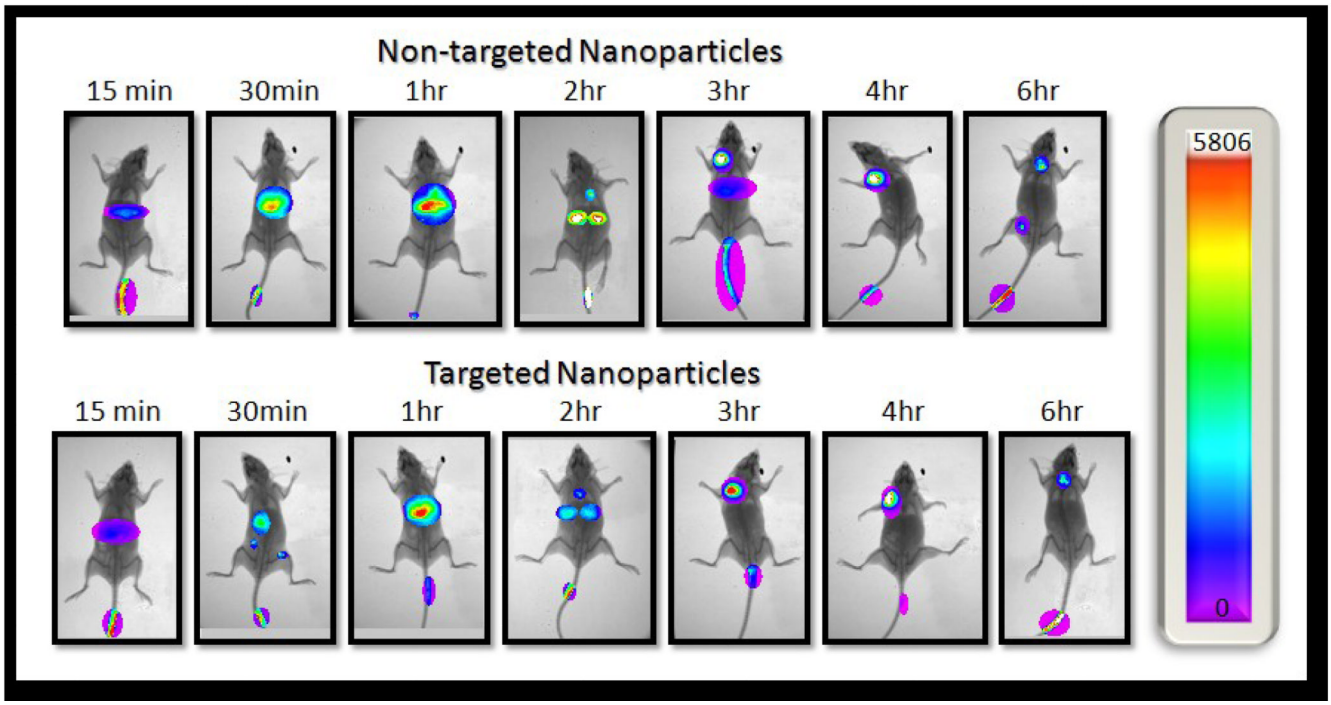

Figure 4.

Biodistribution of Non-targeted and Targeted Nanoparticles Loaded with DiR. Each image represents an overlay of the X-ray and fluorescent fields. The intensity of each fluorescent region corresponds to the scale on the right hand side, with the white regions displaying the highest intensity and the purple regions representing an intensity of zero (background); purple regions (background) surround most regions of interest. The organs are labeled as follows; L = Liver, K = Kidney, and T = Tumor.

Table 1

Plasma Pharmacokinetic Parameters[§]

Drug[¶]	Treatment[#]	λ_z	$T_{½}$	T_{max}	C_{max}	$AUC_{0-\infty}$	$AUMC_{0-\infty}$	$MRT_{0-\infty}$	Cl_t	V_d
PTX	SOL	0.66 ± 0.13	1.05 ± 0.33	1	146 ± 14.37	508.74 ± 10.81	825.39 ± 22.71	1.62 ± 0.88	0.04 ± 0.01	0.06 ± 0.03
PTX	TAR NP	0.36 ± 0.07 *	1.92 ± 0.26	1	107.04 ± 11.04	497.60 ± 17.46	1364.85 ± 31.64 ***	2.74 ± 0.75	0.040 ± 0.02	0.11 ± 0.09
PTX	NON NP	0.34 ± 0.10**	2.06 ± 0.50	1	102.48 ± 16.84	436.48 ± 12.36**/‡	1201.23 ± 29.04***/###	2.75 ± 0.77	0.05 ± 0.01	0.13 ± 0.09
LON	SOL	0.42 ± 0.16	1.67 ± 1.32	1	185.33 ± 21.99	768.80 ± 24.75	1815.05 ± 24.52	2.36 ± 0.64	0.10 ± 0.02	0.25 ± 0.11
LON	TAR NP	0.17 ± 0.09	4.16 ± 1.87*	1	207.32 ± 27.81	1316.01 ± 33.07***	5761.99 ± 34.85***	4.38 ± 1.01***	0.06 ± 0.03	0.27 ± 0.18
LON	NON NP	0.18 ± 0.12	3.92 ± 1.42	1	183.37 ± 24.71	992.44 ± 35.46***/###	3738.87 ± 31.66***/###	3.77 ± 1.00	0.08 ± 0.05	0.30 ± 0.14

[§]Parameter (abbreviation, units): the terminal elimination rate constant (λ_Z, 1/h), the half-life ($T_{½}$, h), the time of maximal concentration (T_{max}, h), the maximal concentration (C_{max}, μg/ml), the area under the curve ($AUC_{0-\infty}$, μg/ml*h), the area under the moment cur ($AUMC_{0-\infty}$, μg/ml*h^2), the mean residence time ($MRT_{0-\infty}$, h), the total body clearance (Cl_t, (mg/kg)/(μg/ml)/h), and the volume distribution (V_d, (mg/kg)/(μg/ml)).

[¶]Drug; Paclitaxel (PTX), Lonidamine (LON)

[#]Treatment; Solution (SOL), Targeted Nanoparticles (TAR NP), Nontargeted Nanoparticles (NON NP)

*** $p<0.0001$,

** $p<0.01$,

* $p<0.05$ between SOL and either TAR NP or NON NP

$p<0.0001$,

$p<0.01$,

‡ $p<0.05$ between TAR NP and NON NP

Table 2

Tumor Pharmacokinetic Parameters[§]

Drug[¶]	Treatment[#]	λ_z	$T_{½}$	T_{max}	C_{max}	$AUC_{0-\infty}$	$AUMC_{0-\infty}$	$MRT_{0-\infty}$	Cl_t	V_d
PTX	SOL	0.53 ± 0.17	1.31 ± 1.00	1	1.06 ± 0.72	4.52 ± 3.90	9.72 ± 3.58	2.15 ± 1.22	4.42 ± 1.65	9.50 ± 2.03
PTX	TAR NP	0.08 ± 0.09***	8.24 ± 2.16***	3	3.01 ± 1.06	38.32 ± 13.14**	438.60 ± 23.34***	11.45 ± 3.70***	0.52 ± 0.20	5.98 ± 2.11
PTX	NON NP	0.12 ± 0.11***	5.92 ± 2.49*	3	2.24 ± 1.22	25.57 ± 9.43	198.27 ± 19.08***/‡‡	7.75 ± 2.01***	0.78 ± 0.11	6.06 ± 2.47
LON	SOL	0.63 ± 0.15	1.09 ± 1.20	1	1.15 ± 0.99	4.58 ± 3.65	8.88 ± 2.75	1.94 ± 0.53	17.47 ± 5.64	33.85 ± 7.85
LON	TAR NP	0.13 ± 0.04***	5.39 ± 1.63*	3	7.38 ± 1.84***	49.96 ± 9.87***	362.38 ± 33.59***	7.25 ± 1.38***	1.60 ± 1.19***	11.61 ± 4.94***
LON	NON NP	0.26 ± 0.07**	2.63 ± 1.31	3	5.68 ± 1.30***	32.09 ± 14.26*	142.99 ± 22.65***/‡‡	4.46 ± 1.01	2.49 ± 1.22***	11.11 ± 3.87***

[§]Parameter (abbreviation, units;: the terminal elimination rate constant (λ_Z, 1/h), the half-life ($T_{½}$, h), the time or maximal concentration (T_{max}, h), the maximal concentration (C_{max}, μg/ml), the area under the curve ($AUC_{0-\infty}$, μg/ml*h), the area under the moment curve ($AUMC_{0-\infty}$, μg/ml*h^2), the mean residence time ($MRT_{0-\infty}$, h), the total body clearance (Cl_t,(mg/kg)/(μg/ml)/h), and the volume of distribution (V_d, (mg/kg)/(μg/ml)).

[¶]Drug; Paclitaxel (PTX), Lonidamine (LON)

[#]Treatment; Solution (SOL), Targeted Nanoparticles (TAR NP), Nontargeted Nanoparticles (NON NP)

*** $p<0.0001$,

** $p<0.01$,

* $p<0.05$ between SOL and either TAR NP or NON NP

‡‡‡ $p<0.0001$,

‡‡ $p<0.01$,

‡ $p<0.05$ between TAR NP and NON NP